J Mol Model (2010) 16:1085–1092
DOI 10.1007/s00894-009-0620-0

ORIGINAL PAPER

Calculations of the charge distribution in dodecyltrimethylammonium: a quantum chemical investigation

Benoît Minisini · Sylvain Chavand · Rudolph Barthelery · François Tsobnang

Received: 2 April 2009 / Accepted: 13 October 2009 / Published online: 19 November 2009

Abstract In this work we report the atomic partial charges evaluated on dodecyltrimethylammonium ion. The values obtained from 17 quantum methods [CHELP, CHELPG, MK, NPA at (HF, LDA, PBE, B3LYP)//6-31G++(d,p) level and APT at B3LYP//6-31G++(d,p)] on the molecule optimised at B3LYP/6-31G++(d,p) level were compared to two semiempirical methods (Gasteiger and Qeq) and the commercial force field PCFF. All methods based on quantum calculation gave a positive charge delocalised on at least the first four alkyl groups of the tail. However, those deriving partial charges from the electrostatic potential gave an unrealistic set of alternative positive and negative alkyl group charges along the tail. In comparison, the NPA and APT methods lead to a steady decrease in the partial charges from the third alkyl group, and agreed closely with the representation of the electrostatic potential mapped onto the 0.002 au isodensity surface. The choice of the exchange correlation treatment does not drastically influence the atomic partial charges.

Keywords Dodecyltrimethylammonium · Electrostatic charges · Quantum calculations

Introduction

Since the 1990s there has been a growing interest in cationic surfactants due to their important implications in new technologies such as room temperature ionic liquids [1] or nanomaterials [2]. Also dating from the 1990s, molecular modelling simulations carried out intensively for different purposes have been well detailed in different reviews [2–4]. Among the different methods available, atomistic methods, despite their simulated size and time limitations, are still considered among the most precise techniques with which to study surfactant systems. The main characteristics of the atomistic method rely on accurate treatment of the van der Waals and Coulombic interactions. Therefore, the parameterisation of partial atomic charges is crucial in the evaluation of numerical results when a quantitative comparison with experimental data is required. This statement is illustrated perfectly by the works of Heinz et al., which deal with the experimental determination of the partial atomic charges of silicates [5] and the impact of these partial charges on surface energy calculations [6]. However, to our knowledge, no experimental technique is yet available to measure the electrostatic charges of surfactants. Consequently, numerical methods remain the most accurate means of evaluating these charges. In general, the charges of alkylammonium ions are taken directly from existing force fields such as COMPASS [7–10] or ffgmx [11]. When UFF [12–16] and Dreiding [15–22] force fields are used, the charges are often evaluated using the charge equilibration method [13, 14, 17–21]. Otherwise, the charges for NH_4^+, $CH_3NH_3^+$ and $(CH_3)_4N^+$ evaluated by Jorgensen and Gao [23] in 1986 from a population analysis on wave functions obtained at HF/6-31G* level are used extensively for more recent atomistic simulation studies [24–28]. At the beginning of the nineties, Böcker et al. [29] used the same level of theory to evaluate the charge distribution on ethyltrimethylammonium ion, once again their results were used as a reference for more recent atomistic simulation studies [30, 31]. More recently a method deriving the charge from electrostatic potential calculated at a HF/6-31G* level was used to

B. Minisini (✉) · S. Chavand · R. Barthelery · F. Tsobnang
Institut Supérieur des Matériaux et Mécaniques Avancés du Mans,
44 Av. Bartholdi,
72000 Le Mans, France
e-mail: bminisini@ismans.fr

evaluate the atomic partial charges of hexylammonium [33], hexytrimethylammoium [33], dodecyltrimethylammonium [32, 33] and octyltrimethylammonium [34] ions. However, to our knowledge, the only results including correlation effects were obtained for cetylpiridinium ion [35] from B3LYP/SVP calculations.

These previous studies highlight the wide dispersion of calculated atomic charge values. For example, the nitrogen charges cover a range of values from −0.628e [36] to 0.20e [33] for the alkyltrimethylammonium ion. Moreover, the charges were in some cases calculated only for the headgroup and, consequently, the charges of the alkyl group of the tail were fixed at zero. However, from a study of charge distribution in ionic surfactant performed with semiempirical methods, Huibers [37] have shown that 10% of the positive charge could reside on the tail.

Consequently, the aim of this work was to compare the charge distributions in dodecyltrimethylammonium ion ($CH_3(CH_2)_{11}(CH_3)_3N^+$) obtained with different methods. The wave functions and electrostatic potential determinations were performed using HF, MP2, LDA, GGA, B3LYP theories and the 6–31++G(d,p) basis set on geometry previously optimised with the B3LYP theory and 6–31++G (d,p) basis set. After comparing the electrostatic potential, we compared the atomic partial charges calculated according to three methods: electrostatic potentials, natural population analysis and atomic polar tensor analysis. These results were also compared to those obtained from charge equilibration methods and those available in the COMPASS force field.

Methods

The linear geometry of dodecyltrimethylammonium ion was optimised using the GAUSSIAN98 [38] program at the B3LYP/6–31++g(d,p) level. The self consistent field (SCF) convergence on the density matrix was set to 10^{-8} a.u., whereas the Berny algorithm [39] was used for the optimisation, with the criteria for convergence being a maximum force of less than 45 10^{-5} a.u. and a root mean squares (rms) force less than 3 10^{-4} a.u. The molecular electrostatic potential (MEP) and the atomic population were then evaluated using Hartree-Fock (HF) [40], second order Moller-Plesset perturbation theory (MP2) [41], local density approximation (LDA) [42], generalised gradient approximation (GGA) with the PBE [43] exchange correlation functional and B3LYP [44, 45] hybrid exchange correlation functional with 6–31++g(d,p) basis set, on the previously optimised geometry using the GAUSSIAN03 [46] program. Population analyses were first evaluated using three methods based on the fit of the MEP under the constraint of reproducing the dipole moment. The CHELP [47] method was used with the atomic radii defined by Francl and five shells leading to 2,892 points to fit. The CHELPG [48] method was used with the atomic radii defined by Breneman. The grid spacing and the outer grid radius were 0.3 Bohr and 2.8 Bohr, respectively, resulting in 25,882 points to fit. Concerning the MK [49, 50] method, four shells, with scaling factors ranging from 1.4 to 2, were used around the van der Waals envelope defined by the Merz-Kollman atomic radii. The default density of grid points provided 1,861 points to use for the fitting. Natural population analysis (NPA) [51, 52] and Cioslowki's atomic polar tensor (APT) [53, 54] were also considered. These results were compared to less demanding methods such as the charge equilibration methods available in the Materials Studio software package (version 4.2) [55]. The Qeq_charge 1.1 [56] and Gasteiger 1.0 [57] methods were used with a convergence limit of 5×10^{-6} |e|.

Results and discussion

The structure of the optimised dodecyltrimethylammonium ion and the MEP mapped on the electron density surface is presented in Fig. 1. An isodensity value of 0.002 e/Bohr^3 was chosen. This mapped surface was created from the results obtained at B3LYP level with a colour scale varying from 0 kcal mol^{-1} (red) to 127 kcal mol^{-1} (blue). From these results, the molecule can be divided clearly into three parts. The blue region on the right represents an important electrophilic region with a large positive electrostatic potential. This region includes the nitrogen atoms, the three methyl groups and the two first alkyl groups of the tail. The second region (in green) spreading from Met2 to Met7 means that the electrostatic potential is significantly positive in this area. The colour in the last region, including the rest of the tail,

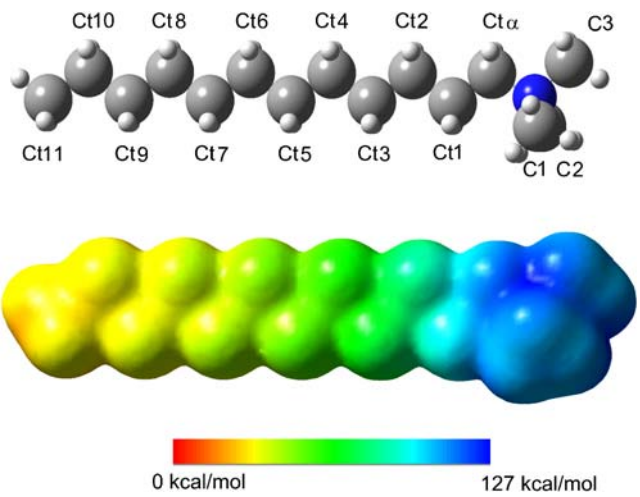

Fig. 1 Mapping of the electrostatic potential onto the electron density surface (0.002 e/bohr^3) evaluated at B3LYP//6−31G++(d,p) level. *Blue* More electrophilic regions, *red* less electrophilic regions

Table 1 Atomic partial charges calculated within the framework of density functional theory (DFT)

		LDA-6–31++G(d,p)				PBE-6–31++G(d,p)				B3LYP-6–31++G(d,p)				
		MK	CHELP	CHELPG	NPA	MK	CHELP	CHELPG	NPA	MK	CHELP	CHELPG	NPA	APT
N	N	0.05	0.23	0.14	−0.29	0.10	0.26	0.17	−0.31	0.11	0.27	0.18	−0.33	−0.43
C_1	C_1	−0.41	−0.09	−0.28	−0.54	−0.38	−0.07	−0.25	−0.48	−0.35	−0.05	−0.22	−0.45	0.17
H_{1a}	H_{1a}	0.21	0.08	0.16	0.29	0.19	0.07	0.14	0.27	0.18	0.06	0.13	0.26	0.04
H_{1b}	H_{1b}	0.23	0.10	0.17	0.29	0.21	0.09	0.16	0.27	0.20	0.08	0.15	0.26	0.05
H_{1c}	H_{1c}	0.20	0.09	0.16	0.29	0.19	0.08	0.14	0.27	0.18	0.08	0.13	0.26	0.05
C_2	C_2	−0.41	−0.08	−0.28	−0.54	−0.38	−0.06	−0.25	−0.48	−0.35	−0.05	−0.22	−0.45	0.17
H_{2a}	H_{2a}	0.23	0.10	0.17	0.29	0.21	0.09	0.16	0.27	0.20	0.08	0.15	0.26	0.05
H_{2b}	H_{2b}	0.21	0.08	0.16	0.29	0.19	0.07	0.14	0.27	0.18	0.06	0.13	0.26	0.04
H_{2c}	H_{2c}	0.21	0.09	0.16	0.29	0.19	0.08	0.14	0.27	0.18	0.08	0.13	0.26	0.05
C_3	C_3	−0.53	−0.34	−0.32	−0.54	−0.48	−0.30	−0.28	−0.48	−0.45	−0.28	−0.25	−0.45	0.19
H_{3a}	H_{3a}	0.24	0.15	0.17	0.29	0.22	0.13	0.15	0.27	0.21	0.12	0.14	0.26	0.05
H_{3b}	H_{3b}	0.24	0.15	0.17	0.29	0.22	0.13	0.15	0.27	0.21	0.12	0.14	0.26	0.05
H_{3c}	H_{3c}	0.25	0.18	0.17	0.29	0.23	0.16	0.16	0.27	0.22	0.15	0.15	0.26	0.04
C_α	C	−0.24	0.08	−0.19	−0.30	−0.21	0.09	−0.16	−0.26	−0.19	0.10	−0.15	−0.23	0.34
H_α	H	0.16	0.02	0.12	0.28	0.14	0.02	0.11	0.27	0.14	0.01	0.10	0.26	0.00
H_α	H	0.16	0.02	0.12	0.28	0.14	0.02	0.11	0.27	0.14	0.01	0.10	0.26	0.00
C_{t1}	C	0.04	0.18	0.07	−0.54	0.05	0.19	0.08	−0.50	0.06	0.20	0.09	−0.48	0.00
H_{t1}	H	0.05	−0.06	0.02	0.27	0.04	−0.06	0.01	0.25	0.03	−0.07	0.01	0.24	−0.01
H_{t1}	H	0.05	−0.06	0.02	0.27	0.04	−0.06	0.01	0.25	0.03	−0.07	0.01	0.24	−0.01
C_{t2}	C	−0.08	−0.08	0.00	−0.51	−0.05	−0.05	0.03	−0.47	−0.04	−0.04	0.04	−0.45	0.13
H_{t2}	H	0.05	0.01	0.02	0.26	0.04	0.00	0.01	0.25	0.03	−0.01	0.00	0.23	−0.03
H_{t2}	H	0.05	0.01	0.02	0.26	0.03	0.00	0.01	0.25	0.03	−0.01	0.00	0.23	−0.03
C_{t3}	C	−0.06	0.19	−0.07	−0.51	−0.04	0.20	−0.05	−0.47	−0.02	0.22	−0.03	−0.45	0.11
H_{t4}	H	0.03	−0.04	0.02	0.26	0.02	−0.05	0.01	0.24	0.01	−0.05	0.00	0.23	−0.04
H_{t4}	H	0.03	−0.04	0.02	0.26	0.02	−0.05	0.01	0.24	0.01	−0.05	0.01	0.23	−0.04
C_{t15}	C	0.06	0.07	0.04	−0.51	0.08	0.09	0.06	−0.47	0.09	0.10	0.07	−0.45	0.10
H_{t5}	H	0.00	−0.04	0.00	0.26	−0.01	−0.05	−0.01	0.24	−0.02	−0.06	−0.02	0.23	−0.04
H_{t5}	H	0.00	−0.04	0.00	0.26	−0.01	−0.05	−0.01	0.24	−0.02	−0.06	−0.02	0.23	−0.04
C_{t6}	C	−0.05	0.05	0.02	−0.51	−0.03	0.07	0.04	−0.47	−0.01	0.09	0.06	−0.44	0.10
H_{t6}	H	0.02	−0.05	0.00	0.26	0.00	−0.06	−0.01	0.24	0.00	−0.06	−0.02	0.23	−0.05
H_{t6}	H	0.02	−0.05	0.00	0.26	0.00	−0.06	−0.01	0.24	0.00	−0.06	−0.02	0.23	−0.05
C_{t7}	C	−0.01	0.24	0.00	−0.51	0.01	0.25	0.02	−0.47	0.02	0.27	0.04	−0.44	0.11
H_{t7}	H	0.01	−0.07	0.00	0.26	0.00	−0.08	−0.01	0.24	−0.01	−0.09	−0.02	0.22	−0.05
H_{t7}	H	0.01	−0.07	0.00	0.26	0.00	−0.08	−0.01	0.24	−0.01	−0.09	−0.02	0.22	−0.05
C_{t8}	C	0.08	0.06	0.07	−0.51	0.09	0.08	0.09	−0.47	0.10	0.09	0.10	−0.44	0.10
H_{t8}	H	−0.01	−0.04	−0.02	0.25	−0.02	−0.05	−0.03	0.24	−0.03	−0.06	−0.03	0.22	−0.05
H_{t8}	H	−0.01	−0.04	−0.02	0.25	−0.02	−0.05	−0.03	0.24	−0.03	−0.06	−0.03	0.22	−0.05

Table 1 (continued)

		LDA-6–31++G(d,p)				PBE-6–31++G(d,p)				B3LYP-6–31++G(d,p)				
		MK	CHELP	CHELPG	NPA	MK	CHELP	CHELPG	NPA	MK	CHELP	CHELPG	NPA	APT
C_{t9}	C	−0.09	0.01	−0.04	−0.51	−0.06	0.04	−0.02	−0.47	−0.05	0.06	0.00	−0.44	0.11
H_{t9}	H	0.02	−0.04	0.00	0.25	0.01	−0.05	−0.01	0.24	0.00	−0.05	−0.02	0.22	−0.05
H_{t9}	H	0.02	−0.04	0.00	0.25	0.01	−0.05	−0.01	0.24	0.00	−0.05	−0.02	0.22	−0.05
C_{t10}	C	−0.03	0.19	−0.01	−0.51	−0.01	0.21	0.01	−0.47	0.01	0.22	0.03	−0.45	0.10
H_{t10}	H	0.01	−0.06	0.00	0.25	0.00	−0.07	−0.01	0.24	−0.01	−0.08	−0.02	0.22	−0.05
H_{t10}	H	0.01	−0.06	0.00	0.25	0.00	−0.07	−0.01	0.24	−0.01	−0.08	−0.02	0.22	−0.05
C_{t11}	C	0.16	0.18	0.16	−0.51	0.18	0.19	0.17	−0.48	0.19	0.20	0.18	−0.45	0.13
H_{t11}	H	−0.02	−0.06	−0.02	0.25	−0.03	−0.07	−0.03	0.24	−0.04	−0.08	−0.04	0.22	−0.05
H_{t11}	H	−0.02	−0.06	−0.02	0.25	−0.03	−0.07	−0.03	0.24	−0.04	−0.08	−0.04	0.22	−0.05
C_{t12}	C	−0.32	−0.12	−0.25	−0.75	−0.27	−0.08	−0.20	−0.69	−0.25	−0.06	−0.18	−0.66	0.08
H_{t12}	H	0.08	0.01	0.06	0.25	0.06	0.00	0.04	0.23	0.05	−0.01	0.03	0.22	−0.03
H_{t12}	H	0.08	0.01	0.06	0.25	0.06	0.00	0.04	0.23	0.05	−0.01	0.03	0.22	−0.03
H_{t12}	H	0.09	0.05	0.07	0.26	0.07	0.03	0.05	0.24	0.06	0.02	0.04	0.23	−0.04

ranges from greenish-yellow to orange-yellow. Consequently, even if it is close to zero, the electrostatic potential remains positive even far from the headgroup. The same division is visible from the results obtained with the two ab initio methods and the three density functional theory (DFT) methods. However, the net maximal value of the positive electrostatic potential (V_{max}) differs as a function of the methods. For an isodensity value of 0.002 e/bohr^3, V_{max} ranges from 124 kcal mol^{-1} to 132 kcal mol^{-1}. The most positive values are obtained for the HF methods. The value of V_{max} is also basis set dependent since V_{Max} obtained at the HF/6–31g(d) level is 3 kcal mol^{-1} higher than the value obtained at the HF/6–31g++(d) level. The lowest value of V_{max} is obtained with the LDA calculation whereas GGA and hybrid results are close together.

Tables 1 and 2 present the atomic partial charges evaluated with the different methods. The results obtained with the HF/6–31G(d) are not presented but can be obtained from the authors on request. As observed in previous studies [33, 36], the sign of the nitrogen partial charge depends on the method of evaluation. Thus, all the methods based on the fitting of the electrostatic potential gave a positive nitrogen value, varying from 0.05|e| to 0.32|e| respectively for the MK scheme at the LDA-6.31++G(d,p) level and the CHELP scheme at the HF-6–31++G(d,p) level. The CHELPG nitrogen charge is, on average from the chemistry models, 0.1|e| and 0.17|e| more positive than the values obtained with the CHELP and the MK schemes. This difference is not due to a poor fitting technique since, for all these methods, the maximum rms and the relative rms (rrms) are small, with the most important value being 0.00233 u.a. and 0.02751%, respectively. This discrepancy has already been reported [58] and can be attributed to the different van der Waals radii used in the three schemes—the nitrogen van der Waals radius is 1.50, 1.67 and 1.70 Bohr for the MK, CHELP and CHELPG methods, respectively—and the choice of the points used in the least-squares fit of the electrostatic potential. More recent methods such as CHELP-BOW [59] could be tested to see the effect of the inclusion of fit potential points inside the van der Waals surface. On the other hand, the nitrogen charges evaluated by NPA and APT are negative. However, the calculated values are less negative than the atomic charges used in commercial force fields. Concerning the charge of the carbon atoms in the methyl groups, all the methods except APT give negative values. We also note that the NPA method is the only method that does not make the distinction between the three methyl groups. In all the others methods, the atomic charges of the two methyl groups that are equivalent by mirror symmetry and which include C_1 and C_2 carbon atoms are the same, and differ from the methyl group that includes the C_3 carbon atom. The negative atomic charges on the nitrogen and carbon

Table 2 Atomic partial charges calculated at the Hartree Fock (HF) and post-HF level of theory, the semi empirical level and given by commercial force field

	HF-6–31++G(d,p)				MP2-6–31++G(d,p)				Semi empirical		Force field
	MK	CHELP	CHELPG	NPA	MK	CHELP	CHELPG	NPA	Gasteiger	Qeq	COMPASS
N	0.15	0.32	0.22	−0.41	0,15	0,32	0,22	−0,41	0.14	−0.40	−0.628
C_1	−0.38	−0.08	−0.25	−0.37	−0,38	−0,08	−0,25	−0,37	0.02	−0.25	0.248
H_{1a}	0.19	0.07	0.14	0.24	0,19	0,07	0,14	0,24	0.06	0.15	0.053
H_{1b}	0.21	0.09	0.15	0.24	0,21	0,09	0,15	0,24	0.06	0.15	0.053
H_{1c}	0.19	0.08	0.14	0.24	0,19	0,08	0,14	0,24	0.06	0.15	0.053
C_2	−0.38	−0.08	−0.25	−0.37	−0,38	−0,08	−0,25	−0,37	0.02	−0.25	0.248
H_{2a}	0.21	0.09	0.16	0.24	0,21	0,09	0,15	0,24	0.06	0.16	0.053
H_{2b}	0.19	0.07	0.14	0.24	0,19	0,07	0,14	0,24	0.06	0.15	0.053
H_{2c}	0.19	0.08	0.14	0.24	0,19	0,08	0,14	0,24	0.06	0.15	0.053
C_3	−0.51	−0.33	−0.28	−0.37	−0,51	−0,33	−0,28	−0,37	0.02	−0.27	0.248
H_{3a}	0.22	0.13	0.15	0.24	0,22	0,13	0,15	0,24	0.06	0.15	0.053
H_{3b}	0.22	0.13	0.15	0.24	0,22	0,13	0,15	0,24	0.06	0.16	0.053
H_{3c}	0.23	0.16	0.16	0.24	0,23	0,16	0,16	0,24	0.06	0.16	0.053
C_α	−0.23	0.11	−0.17	−0.17	−0,23	0,11	−0,17	−0,17	0.04	−0.13	0.301
H_α	0.15	0.01	0.11	0.24	0,15	0,01	0,11	0,24	0.07	0.16	0.053
H_α	0.15	0.01	0.11	0.24	0,15	0,01	0,11	0,24	0.07	0.16	0.053
C_{t1}	0.07	0.20	0.10	−0.44	0,07	0,20	0,10	−0,44	−0.02	−0.28	−0.106
H_{t1}	0.03	−0.07	0.00	0.22	0,03	−0,07	0,00	0,22	0.03	0.16	0.053
H_{t1}	0.03	−0.07	0.00	0.22	0,03	−0,07	0,00	0,22	0.03	0.16	0.053
C_{t2}	−0.05	−0.05	0.04	−0.41	−0,05	−0,05	0,04	−0,41	−0.05	−0.31	−0.106
H_{t2}	0.03	0.00	0.00	0.22	0,03	0,00	0,00	0,22	0.03	0.17	0.053
H_{t2}	0.03	0.00	0.00	0.22	0,03	0,00	0,00	0,22	0.03	0.17	0.053
C_{t3}	−0.03	0.21	−0.05	−0.41	−0,03	0,21	−0,05	−0,41	−0.05	−0.29	−0.106
H_{t4}	0.01	−0.05	0.01	0.21	0,01	−0,05	0,01	0,21	0.03	0.17	0.053
H_{t4}	0.01	−0.05	0.01	0.21	0,01	−0,05	0,01	0,21	0.03	0.17	0.053
C_{t15}	0.09	0.10	0.07	−0.41	0,09	0,10	0,07	−0,41	−0.05	−0.29	−0.106
H_{t5}	−0.02	−0.06	−0.02	0.21	−0,02	−0,06	−0,02	0,21	0.03	0.17	0.053
H_{t5}	−0.02	−0.06	−0.02	0.21	−0,02	−0,06	−0,02	0,21	0.03	0.17	0.053
C_{t6}	−0.02	0.07	0.05	−0.41	−0,02	0,07	0,05	−0,41	−0.05	−0.30	−0.106
H_{t6}	0.00	−0.06	−0.02	0.21	0,00	−0,06	−0,02	0,21	0.03	0.17	0.053
H_{t6}	0.00	−0.06	−0.02	0.21	0,00	−0,06	−0,02	0,21	0.03	0.17	0.053
C_{t7}	0.02	0.26	0.03	−0.41	0,02	0,26	0,03	−0,41	−0.05	−0.29	−0.106
H_{t7}	−0.01	−0.08	−0.02	0.21	−0,01	−0,08	−0,02	0,21	0.03	0.17	0.053
H_{t7}	−0.01	−0.08	−0.02	0.21	−0,01	−0,08	−0,02	0,21	0.03	0.17	0.053
C_{t8}	0.10	0.09	0.10	−0.41	0,10	0,09	0,10	−0,41	−0.05	−0.30	−0.106
H_{t8}	−0.03	−0.05	−0.03	0.20	−0,03	−0,05	−0,03	0,20	0.03	0.17	0.053
H_{t8}	−0.03	−0.05	−0.03	0.20	−0,02	−0,05	−0,03	0,20	0.03	0.17	0.053

Table 2 (continued)

	HF-6–31++G(d,p)				MP2-6–31++G(d,p)				Semi empirical		Force field
	MK	CHELP	CHELPG	NPA	MK	CHELP	CHELPG	NPA	Gasteiger	Qeq	COMPASS
C_{t9}	−0.07	0.03	−0.02	−0.41	−0,06	0,03	−0,02	−0,41	−0.05	−0.30	−0.106
H_{t9}	0.00	−0.05	−0.01	0.20	0,00	−0,05	−0,01	0,20	0.03	0.17	0.053
H_{t9}	0.00	−0.05	−0.01	0.20	0,00	−0,05	−0,01	0,20	0.03	0.17	0.053
C_{t10}	0.00	0.22	0.03	−0.41	0,00	0,22	0,03	−0,41	−0.05	−0.28	−0.106
H_{t10}	0.00	−0.07	−0.01	0.20	0,00	−0,07	−0,01	0,20	0.03	0.18	0.053
H_{t10}	0.00	−0.07	−0.01	0.20	0,00	−0,07	−0,01	0,20	0.03	0.18	0.053
C_{t11}	0.19	0.20	0.19	−0.42	0,19	0,20	0,18	−0,42	−0.06	−0.30	−0.106
H_{t11}	−0.03	−0.07	−0.04	0.20	−0,03	−0,07	−0,04	0,20	0.03	0.18	0.053
H_{t11}	−0.03	−0.07	−0.04	0.20	−0,03	−0,07	−0,04	0,20	0.03	0.18	0.053
C_{t12}	−0.28	−0.09	−0.21	−0.60	−0,28	−0,09	−0,21	−0,60	−0.07	−0.41	−0.159
H_{t12}	0.06	−0.01	0.04	0.20	0,06	−0,01	0,04	0,20	0.02	0.17	0.053
H_{t12}	0.06	−0.01	0.04	0.20	0,06	−0,01	0,04	0,20	0.02	0.17	0.053
H_{t12}	0.07	0.03	0.05	0.21	0,07	0,03	0,05	0,21	0.02	0.17	0.053

atoms, and the distinction between the three methyl groups do not agree with the distribution of the electrostatic potential visible in Fig. 1. The electrostatic potential is positive all around the headgroup; consequently, we expected to have a positive atomic charge on all the atoms present in the headgroup. Moreover, the potential is more positive close to the nitrogen atom compared to near the hydrogen atoms but all the methods gave a smaller atomic charge on the nitrogen atom than on the hydrogen atoms.

From a more global point of view, it is interesting to evaluate the global charge of the headgroup and to compare this value with the common model using a point unit charge at the headgroup. The α methylene group linking the headgroup to the tail has been included in the reported values. It appears that the charge is less than 1|e| for all the methods used. With the exception of the exceptionally low value of 0.379|e| obtained with the semi empirical method Qeq, the charges range from 0.78|e| to 0.95|e|. This latter value, calculated with the other semiempirical method Gasteiger1.0, was relatively close to that evaluated with the NPA method, which ranged from 0.92|e| to 0.93|e|. The charges calculated from the APT and CHELP methods ranged from 0.85|e| to 0.87|e| and, finally, the MK and CHELPG methods gave some values between 0.77|e| and 0.80|e|. In general, for the same method of calculation, the charges were in the following order: HF>B3LYP>P-BE>LDA. The CHELP method is sensitive to the exchange correlation term, with a maximal difference of 0.02|e|, in contrast to the NPA method with a difference of less than 0.009|e|. Consequently, we can say that the charge of the headgroup is more sensitive to the way atomic charges are determined than to the quantum chemical model. The largest discrepancy is that of 17% between the MK charges and the NPA evaluated at the B3LYP level. It is difficult to determine if one method is better than another, but we can be sure that such a large difference in charge affects the solubility of the molecule. Compared to a point unit charge model, all of the calculations lead to a delocalisation of the positive charge on the tail, as observed by Huibers [37], owing to semiempirical quantum calculation. To evaluate the expansion of this distribution, we plotted the distribution of the alkyl groups charges along the tail.

Figure 2 represents the distribution of the charges estimated from the electrostatic potential evaluated at the B3LYP level, the other results give a similar shape with slightly different charges and are thus not represented for better visibility. We can see that the least square fit led to an odd-even effect, with a set of alternative positive and negative alkyl group charges. This behaviour seems unrealistic compared to the electrostatic potential steadily decreasing along the tail. The concept of charge alternation arose from evidence presented by Pople and Gordon [60] at the end of the 1960s. Poltizer et al. [61] reviewed the

controversial experimental and numerical data of the 1970s and performed some calculations on fluorine hydrocarbon at the beginning of the 1980s. Relying on this review, their results and the work of Weinstein et al. [62], Poltizer et al. concluded that alternating atomic charges are not inconsistent with an electrostatic potential without sign of alternation. Moreover, if we sum up the partial charges of the first four alkyl groups, we find charges of 0.19|e|, 0.16|e| and 0.11|e| for the MK, CHELPG and CHELP methods, respectively. The sum of the partial charges on Met5, Met6 and Met7 was close to 0.3|e| for all the methods, whereas the sum of the last four alkyl groups led to a charge of 0|e|. Consequently, even if the partial charges of the alkyl group seemed wrong, the distribution of the charge along the tail was consistent with the electrostatic potential.

This delocalisation is also visible in Fig. 3, which represents the distribution of the partial charge evaluated with the APT and NPA methods. The evolution of the charge along the tail was very similar, whereas the methods differ completely from a technical point of view. In both cases, we had a low partial charge on Met1 and then a greater charge on Met2 followed by a steady decrease in the partial charges until Met8. As in Fig. 2, we can see an odd–even effect but only on the last four methyl groups. The sums of the partial charges on the last four alkyl groups were 0.02|e| and 0.01|e| for APT and NPA, respectively. This result is in agreement with the positive electrostatic potential visible at the end of the tail in Fig. 1.

As expected, the partial charges given in commercial force fields did not take into account the distribution of the positive charge on the tail (Fig. 4). The semiempirical method Gasteiger gave a positive charge delocalised on the first two alkyl groups whereas Qeq delocalised more than 60% of the charge all along the tail, the last alkyl group having a charge higher than 0.10|e|. Consequently, from these results, the Qeq method did not seem appropriate for the evaluation of the atomic partial charge in dodecyltrimethylammonium.

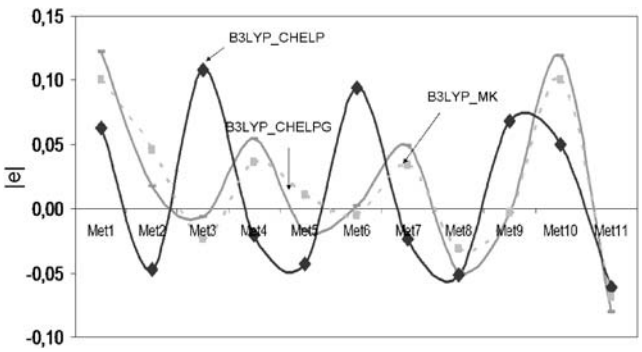

Fig. 2 Distribution of the derived partial charges from electrostatic potential along the alkyl tail. Met_X stands for the Xth methylene group composed of C_{tX} and the two H_{tX} atoms defined in Tables 1 and 2

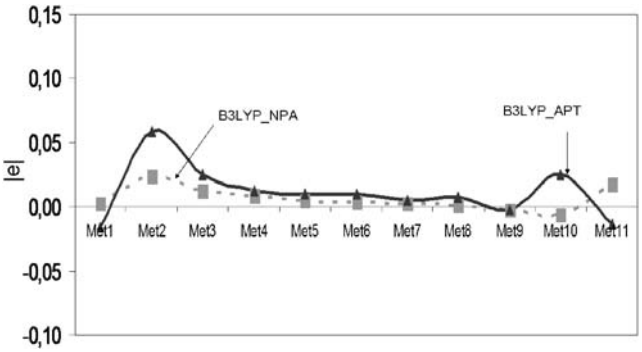

Fig. 3 Distribution of partial charges estimated from natural population analysis (NPA) and Cioslowki's atomic polar tensor (APT) along the alkyl tail

Considering the results as a whole, it is obvious that all the methods tested provided different distributions of the partial charges. However, it is hard to conclude which method is best due to the difficulty in determining the quality criteria. Nevertheless, these partial charges are intended to be used as input parameters in atomistic simulations. Consequently, it would be interesting to see if the discrepancies induced by the different models of atomic partial charges are within the range of statistical error generated by molecular dynamic simulations.

Conclusions

The electrostatic potential of the dodecyltrimethylammonium ion was evaluated at different level for various theories. The influence of the methods for deriving atomic charges from the electrostatic potential was then analysed. The results were compared to other quantum techniques, NPA, Cioslowki's APT, and semi empirical methods. From the electrostatic potential, the molecule can be divided clearly into three parts in function of the values ranging from 0 to 127 kcal mol^{-1}. The partial charges evaluated with the NPA and APT methods represent quite well the steady decrease in the

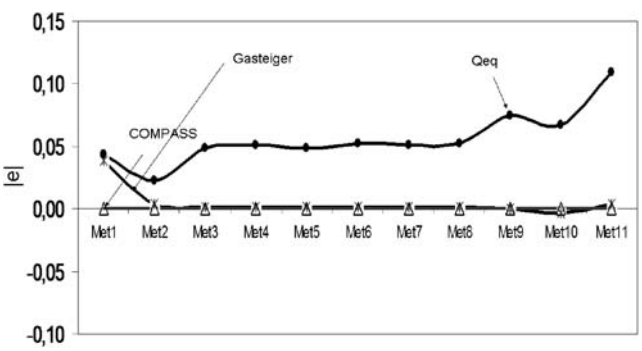

Fig. 4 Distribution of partial charges estimated from the semiempirical method Qeq and Gasteiger and available in the COMPASS force field

electrostatic potential along the tail. The same is true for the methods based on fitting of the electrostatic potential, which give some unrealistic negative partial charges along the tail. It is clear from the results that the different methods provide different estimations of the atomic charges. However, further investigations are now necessary to assess the influence of these different distributions of charge on the results obtained with atomistic simulation.

References

1. Welton T (1999) Chem Rev 99:2071–2083
2. Holmberg K (2003) J Colloid Interface Sci 274:355–364
3. Rajagopalan R (2001) Curr Opin Colloid Interface Sci 6:357–365
4. Li YM XGY, Chen YJ, Luan YX, Yuan SL (2006) Comp Mat Sci 36:386–396
5. Heinz H, Suter UW (2004) J Phys Chem B 108:18341–18352
6. Heinz H, Vaia RA, Farmer BL (2006) J Chem Phys 124:2247131–2247139
7. He H, Galy J, Gerard JF (2005) J Phys Chem B 109:13301–13306
8. Minisini B, Tsobnang F (2005) Compos Part A 36:531–537
9. Yuan S, Ma L, Zhang X, Zheng L, Chen Y, Xu G (2006) Colloids Surf A 289:1–9
10. Yuan S, Chen Y, Xu G (2006) Colloids Surf A 280:108–115
11. Piotrovskaya EM, Vanin AA, Smirnova NA (2006) Mol Phys 104:3645–3651
12. Martynkova GS, Valaskova M, Capkova P, Matejka V (2007) J Colloid Interface Sci 313:281–287
13. Pospisil M, Capkova P, Merinska D, Malac Z, Simonik J (2001) J Colloid Interface Sci 236:127–131
14. Capkova P, Pospisil M, Weiss Z (2003) J Mol Model 9:195–205
15. Gardebien F, Gaudel-Siri A, Bredas JL, Lazzaroni R (2004) J Phys Chem B 108:10678–10686
16. Gardebien F, Bredas JL, Lazzaroni R (2005) J Phys Chem B 109:12287–12296
17. Jang SS, Goddard WA III (2006) J Phys Chem B 110:7992–8001
18. Zeng QH, Yu AB, Lu GQ, Standish RK (2003) Chem Mater 15:4732–4738
19. Zeng QH, Yu AB, Lu GQ, Standish RK (2004) J Phys Chem B 108:10025–10033
20. Paul DR, Zeng QH, Yu AB, Lu GQ (2005) J Colloid Interface Sci 292:462–468
21. Tanaka G, Goettler L (2002) Polymer 43:541–553
22. Zeng QH, Yu A, Lu G (2005) Nanotechnology 16:2757–2763
23. Jorgensen WL, Gao J (1986) J Phys Chem 90:2174–2182
24. Bandyopadhyay S, Shelley JC, Tarek M, Moore PB, Klein ML (1998) J Phys Chem B 102:6318–6322
25. Tarek M, Tobias DJ, Klein ML (1995) J Phys Chem 99:1393–1402
26. Adolf DB, Tideslsey DJ, Pinches MRS, Kingdon JB, Madden T, Clark A (1995) Langmuir 11:237–246
27. Shah K, Chiu P, Jain M, Fortes J, Moudgil B, Sinnott S (2005) Langmuir 21:5337–5342
28. Kong YC, Tildesley DJ, Alejandre J (1997) Mol Phys 92:7–18
29. Böcker J, Schlenkrich M, Bopp P, Brickmann J (1992) J Phys Chem 96:9915–9922
30. Dos Santos DJVA, Gomes JANF (2004) Progr Colloid Polym Sci 126:68–73
31. Böcker J, Brickmann J, Bopp P (1994) J Phys Chem 98:712–717
32. Zanuy D, Casanovas J, Aleman C (2004) Chem Phys 305:85–93
33. Zanuy D, Aleman C (2003) Langmuir 19:3987–3995
34. Zanuy D, Aleman C, Munoz-Guerra S (2002) Biopolymers 63:151–162
35. Meleshyn A, Bunnenberg C (2006) J Phys Chem B 110:2271–2277
36. Teppen BJ, Rasmussen K, Bertsch PM, Miller DM, Schafer L (1997) J Phys Chem B 101:1579–1587
37. Huibers PDT (1999) Langmuir 15:7546–7550
38. Frisch MJ, Trucks GW, Schlegel HB, Scuseria GE, Robb MA, Cheeseman JR, Zakrzewski VG, Montgomery JA Jr, Stratmann RE, Burant JC, Dapprich S, Millam JM, Daniels AD, Kudin KN, Strain MC, Farkas O, Tomasi J, Barone V, Cossi M, Cammi R, Mennucci B, Pomelli C, Adamo C, Clifford S, Ochterski J, Petersson GA, Ayala PY, Cui Q, Morokuma K, Malick DK, Rabuck AD, Raghavachari K, Foresman JB, Cioslowski J, Ortiz JV, Baboul AG, Stefanov BB, Liu G, Liashenko A, Piskorz P, Komaromi I, Gomperts R, Martin RL, Fox DJ, Keith T, Al-Laham MA, Peng CY, Nanayakkara A, Gonzalez C, Challacombe M, Gill PMW, Johnson B, Chen W, Wong MW, Andres JL, Gonzalez C, Head-Gordon M, Replogle ES, Pople JA (1998) Gaussian 98, Revision A7. Gaussian Inc, Pittsburgh, PA
39. Peng C, Ayala PY, Schlegel HB, Frisch MJ (1996) J Comput Chem 17:49–56
40. Roothaan CCJ (1951) Rev Mod Phys 23:69–89
41. Moller C, Plesset MS (1934) Phys Rev B 46:618–622
42. Vosko SH, Wilk L, Nusair M (1980) Can J Phys 58:1200–1211
43. Perdew JP, Buke K, Ernerhof M (1996) Phys Rev Lett 77:3865–3868
44. Becke AD (1993) J Chem Phys 98:5648–5652
45. Lee C, Yang W, Parr RG (1988) Phys Rev B 37:785–789
46. Frisch MJ, Trucks GW, Schlegel HB, Scuseria GE, Robb MA, Cheeseman JR, Montgomery JA Jr, Vreven T Kudin KN, Burant JC, Millam JM, Iyengar SS, Tomasi J, Barone V, Mennucci B, Cossi M, Scalmani G, Rega N, Petersson GA, Nakatsuji H, Hada M, Ehara M, Toyota K, Fukuda R, Hasegawa J, Ishida M, Nakajima T, Honda Y, Kitao O, Nakai H, Klene M, Li X, Knox JE, Hratchian HP, Cross JB, Bakken V, Adamo C, Jaramillo J, Gomperts R, Stratmann RE, Yazyev O, Austin AJ, Cammi R, Pomelli C, Ochterski JW, Ayala PY, Morokuma K, Voth GA, Salvador P, Dannenberg JJ, Zakrzewski VG, Dapprich S, Daniels AD, Strain MC, Farkas O, Malick DK, Rabuck AD, Raghavachari K, Foresman JB, Ortiz JV, Cui Q, Baboul AG, Clifford S, Cioslowski J, Stefanov BB, Liu G, Liashenko A, Piskorz P, Komaromi I, Martin RL, Fox DJ, Keith T, Al-Laham MA, Peng CY, Nanayakkara A, Challacombe M, Gill PMW, Johnson B, Chen W, Wong MW, Gonzalez C, Pople JA (2004) Gaussian 03, Revision C.02. Gaussian Inc, Wallingford CT
47. Chirlian LE, Francl MM (1987) J Comput Chem 8:894–905
48. Breneman CM, Wiberg KB (1990) J Comput Chem 11:361–373
49. Besler BH, Merz KM, Kollman PA (1990) J Comput Chem 11:431–439
50. Singh UC, Kollman PA (1984) J Comput Chem 5:129–145
51. Reed AE, Weinstock RB, Weinhold F (1985) J Chem Phys 83:735–746
52. Reed AE, Curtiss E, Weinstock RB (1988) D Chem Rev 88:899–926
53. Cioslowski J (1989) Phys Rev Lett 62:1469–1471
54. Cioslowski J (1989) J Am Chem Soc 111:8333–8336
55. Accelrys Inc, San Diego (2004) http://accelrys.com/
56. Rappe AK, Goddard WA (1991) J Phys Chem 95:3358–3363
57. Gasteiger J, Marsili M (1980) Tetrahedron 36:3219–3228
58. Masamura M (2000) Struct Chem 11:41–45
59. Sigfridsson E, Ryde U (1998) J Comput Chem 19:377–395
60. Pople JA, Gordon M (1967) J Am Chem Soc 89:4253–4261
61. Politzer P, Whittenburg SLS, Wärnheim T (1982) J Phys Chem 86:2609–2613
62. Weinstein H, Maayani S, Srebenik S, Cohen S, Sokolovsky M (1973) Mol Pharmacol 9:820–834